Published in final edited form as:
Cancer Res. 2011 February 15; 71(4): 1486–1496. doi:10.1158/0008-5472.CAN-10-1343.

Activation of the Androgen Receptor by Intratumoral Bioconversion of Androstanediol to Dihydrotestosterone in Prostate Cancer

James L. Mohler[1,2,3], **Mark A. Titus**[1], **Suxia Bai**[3,4,5], **Brian J. Kennerley**[4], **Fred B. Lih**[6], **Kenneth B. Tomer**[6], and **Elizabeth M. Wilson**[3,4,7]

[1]Department of Urology, Roswell Park Cancer Institute, Buffalo, NY

[2]Department of Urology, University at Buffalo, State University of New York, Buffalo, NY

[3]Lineberger Comprehensive Cancer Center, University of North Carolina, Chapel Hill, NC

[4]Laboratories for Reproductive Biology, Department of Pediatrics, University of North Carolina, Chapel Hill, NC

[6]National Institutes of Environmental Health Sciences, Research Triangle Park, NC

[7]Department of Biochemistry and Biophysics, University of North Carolina, Chapel Hill, NC

Abstract

The androgen receptor (AR) mediates the growth of benign and malignant prostate in response to dihydrotestosterone (DHT). In patients undergoing androgen deprivation therapy for prostate cancer, AR drives prostate cancer growth despite low circulating levels of testicular androgen and normal levels of adrenal androgen. In this report we demonstrate the extent of AR transactivation in the presence of 5α-androstane-3α,17β-diol (androstanediol) in prostate-derived cell lines parallels the bioconversion of androstanediol to DHT. AR transactivation in the presence of androstanediol in prostate cancer cell lines correlated mainly with mRNA and protein levels of 17β-hydroxysteroid dehydrogenase 6 (17β-HSD6), one of several enzymes required for the interconversion of androstanediol to DHT and the inactive metabolite, androsterone. Levels of retinol dehydrogenase 5, and dehydrogenase/reductase short-chain dehydrogenase/reductase family member 9, which also convert androstanediol to DHT, were lower than 17β-HSD6 in prostate-derived cell lines, and higher in the castration-recurrent human prostate cancer xenograft. Measurements of tissue androstanediol using mass spectrometry demonstrated androstanediol metabolism to DHT and androsterone. Administration of androstanediol dipropionate to castration-recurrent CWR22R tumor bearing athymic castrated male mice produced a 28-fold increase in intratumoral DHT levels. AR transactivation in prostate cancer cells in the presence of androstanediol resulted from the cell-specific conversion of androstanediol to DHT, and androstanediol increased LAPC-4 cell growth. The ability to convert androstanediol to DHT provides a mechanism for optimal utilization of androgen precursors and catabolites for DHT synthesis.

Address correspondence to Elizabeth M. Wilson, CB7500, University of North Carolina, Chapel Hill NC 27599-7500, TEL 919-966-5168, FAX 919-966-2203, emw@med.unc.edu.
[5]**Present address**: Janelia Farm Research Campus, Howard Hughes Medical Institute, Ashburn, VA 20147

Potential conflicts of interest: None

Keywords

androgen receptor; prostate cancer; androgen metabolism; dihydrotestosterone; androstanediol; 17β-HSD6

INTRODUCTION

Prostate cancer development and growth depend on the androgen receptor (AR), a ligand-dependent transcription factor required for normal male reproductive function. AR binds testosterone and dihydrotestosterone (DHT) with high affinity to mediate androgen-dependent gene transcription (1). AR is expressed during all stages of prostate cancer progression, and increased AR transcriptional activity is a hallmark of the disease. Inhibition of prostate cancer cell growth by small inhibitory RNAs that target AR provides further evidence for obligatory AR function in prostate cancer development and progression (2).

Prostate cancer growth is stimulated initially by circulating testicular androgens. After treatment by medical or surgical castration, prostate cancers adapt to the androgen-deprived environment to maximize AR function through mechanisms facilitated by the genetic instability of cancer cells. Mechanisms for increased AR transactivation during prostate cancer progression to castration-recurrent growth include AR gene amplification (3), somatic AR gene mutations that provide a gain-of-function by decreasing AR ligand specificity (4,5), and increased AR interactions with coregulators whose levels also increase during prostate cancer progression (6,7). Prostate cancer tissue production of androgen develops during androgen deprivation therapy (8–10), and increased mitogen signaling and AR phosphorylation influences AR transcriptional activity (6,11).

The present study investigated whether AR activation by the conversion of 5α-androstane-3α,17β-diol (androstanediol) to DHT contributes to prostate cancer growth when circulating testicular androgen levels are low. Cell-specific bioactivation of androstanediol to DHT and catabolism to androsterone were investigated as mechanisms for increased AR transcriptional activity that mediates castration-recurrent growth in men undergoing androgen deprivation therapy to treat advanced prostate cancer. Levels of bioavailable DHT reflect activities of several metabolic enzymes. Intracellular DHT derives primarily from the irreversible conversion of testosterone by 5α-reductase. Androstenedione and dehydroepiandrosterone sulfate are major circulating adrenal androgens converted to androstanediol and DHT in human prostate (12). Androstanediol is an inactive DHT metabolite that can be reversibly oxidized to DHT.

Herein we demonstrate AR transcriptional activity in prostate cancer cell lines in the presence of androstanediol is related directly to mRNA and protein levels of 17β-hydroxysteroid dehydrogenase 6 (17β-HSD6) to a greater extent than the retinol dehydrogenase 5 (RDH5), or dehydrogenase/reductase short-chain dehydrogenase/reductase family member 9 (DHRS9), enzymes that convert androstanediol to DHT. Results were corroborated using mass spectrometry to measure DHT and androsterone levels in cells after incubation with androstanediol, and after the administration of androstanediol dipropionate to athymic mice bearing the CWR22R castration-recurrent prostate cancer xenograft. Androstanediol was converted to DHT in the CWR22R xenograft tumor, where mRNA levels were measured for 17β-HSD6, DHRS9 and RDH5. The results support the notion that androstanediol metabolism to DHT coupled with 5α-reductase activity contributes to optimal utilization of androgen precursors and catabolites for AR transactivation during prostate cancer development and progression.

MATERIALS AND METHODS

Human and mouse tissues

Patient specimens of androgen-stimulated benign prostate and androgen-stimulated and castration-recurrent prostate cancer correspond to samples analyzed for AR and melanoma antigen gene protein-A11 mRNA expression (7). Procedures using mice were performed in accordance with the National Institutes of Health and Roswell Park Cancer Institute Institutional Animal Care and Use Committee and Institutional Biosafety Committee. Serially transplanted androgen-dependent CWR22 human prostate cancer xenografts were propagated in athymic nu/nu mice (13) and excised before and at different times after castration for RNA analysis using quantitative real-time PCR (7). To demonstrate intratumoral conversion of androstanediol to DHT, male athymic nude mice 4 to 5 weeks old were purchased from Harlan Sprague Dawley, Inc. (Indianapolis, IN) and housed individually in the Division of Laboratory Animal Research Facility, Roswell Park Cancer Institute. One day after castration, mice were inoculated subcutaneously on one flank with 10^6 CWR22R castration-recurrent xenograft cells suspended in Matrigel (1:1 mixture, BD Biosciences, Bedford, MA). When CWR22R tumors measured 0.5 cm^3, 7 mice were injected subcutaneously at the tumor site with 1 mg androstanediol dipropionate (Steraloids, Newport, RI) in 0.1 mL sesame oil, and 5 mice received vehicle alone. Tumors were excised 2 days later, cut into 0.1 cm^3 pieces, frozen in liquid N_2 and stored at −80°C until analysis using mass spectrometry.

Cell culture, DNA transfection and immunoblot analysis

For AR transcription assays, cells were cultured as described (1,7). CWR-R1 (2×10^5 cells/well of 12 well plates), RWPE-2 (1.5×10^5), LAPC-4 (2×10^5), LNCaP (3.5×10^5), LNCaP-C4-2 (2×10^5) and DU145 cells (1.5×10^5) were transfected using Effectene (Qiagen) with 0.01 μg pCMV-AR and 0.1 μg (CWR-R1 and LAPC-4) or 0.25 μg (RWPE-2, LNCaP, LNCaP-C4-2 and DU145) prostate-specific antigen enhancer luciferase reporter (PSA-Enh-Luc). PWR-1E (2×10^5), PC-3 (1.5×10^5) and HeLa cells (5×10^4) were transfected in 12 well plates using FuGENE 6 (Roche Applied Science) with 0.01 μg pCMV-AR and 0.25 μg PSA-Enh-Luc. CV1 cells (4.2×10^5 cells/6 cm dish) were transfected using calcium phosphate with 0.1 μg pCMV-AR and 5 μg PSA-Enh-Luc. Cells were transferred to serum-free phenol red-free medium 24 h after transfection, and incubated for 24 h with and without testosterone, DHT and androstanediol (Sigma). Cells were washed with phosphate buffered saline and harvested in 0.25 mL (or 0.5 mL for CV1 cells) lysis buffer containing 1% Triton X-100, 2 mM EDTA and 25 mM Tris phosphate, pH 7.8. After rocking for 30 min at room temperature, 0.1 mL aliquots were assayed for luciferase activity using an automated Lumistar Galaxy (BMG Labtech) luminometer.

Immunoblots were performed by plating cells in 10 cm dishes with serum-containing medium to achieve 40 to 60% confluence the next day. After 48 h, cells were scraped into cold phosphate buffered saline, extracted in 0.1 to 0.2 mL lysis buffer containing 1% Triton X-100, 1% deoxycholate, 0.1% SDS, 0.15 M NaCl, 2 mM EDTA, 2 mM sodium vanadate, 0.05 M sodium fluoride, 50 mM Tris-HCl, pH 8.0 and 0.1 μM DHT, and 150 μg protein/lane analyzed on 12% acrylamide gels containing SDS. Nitrocellulose transfer blots were probed using AR52 (10 μg/mL) and AR32 (0.3 μg/mL) antibodies, and HSD17B6 rabbit polyclonal antibody (Abcam ab62221, 1.25 μg/mL). To probe β-actin using a mouse antibody (Abcam, 1:1000 dilution), blots stored at 4°C were stripped at 55°C for 25 min in buffer containing 2% SDS, 92 mM β-mercaptoethanol and 62.5 mM Tris-HCl, pH 6.7. The blot was washed twice for 10 min with 0.15 M NaCl, 0.05% Tween 20 and 10 mM Tris-HCl, pH 7.5, and blocked for 1 h in the same buffer containing 5% nonfat dry milk prior to antibody addition. Immunoreactive bands were visualized by chemiluminescence

(SuperSignal Western Dura Extended Duration substrate, Pierce Biotechnology, Inc., Rockford Ill).

LAPC-4 cell growth assays were performed in triplicate by plating 4×10^4 cells/well of 24 well plates in RPMI-1640 medium containing 10% charcoal stripped fetal bovine serum (Atlanta Biologicals), 20 mM L-glutamine, penicillin and streptomycin. The next day and 48 h later, 0.1 ml serum-free medium was added/well to a final concentration of 0.1 nM DHT and 10 nM androstanediol. Twenty-four h after hormone addition (day 1) and at 24 h intervals, media were aspirated, 0.2 ml fresh serum-free medium and 20 µl WST-8 cell counting reagent (Dojindo Molecular Technologies) were added/well. Cells were incubated for 2.5 h at 37°C and optical density determined at 485 nm. Statistical analysis was performed using the Pearson Product Moment Correlation.

Real-time reverse transcription-PCR

RNA was extracted using TRIzol Reagent (Invitrogen). First strand complementary DNA (cDNA) was prepared using SuperScript II reverse transcriptase (Invitrogen). PCR primers and fluorogenic probe for the constitutive housekeeping gene, peptidylprolyl isomerase A (cyclophilin A) were described (14). Primers and probe for human retinol dehydrogenase 5 (RDH5) (Hs00161263-m1, Applied Biosystems) yield a 126 base pair amplicon spanning exon 3 and 4 junction at assay location nucleotide 681 (NM-002905.2). The 17β-HSD6 primers and probe (Hs00366258-m1, Applied Biosytems) yield a 84 base pair amplicon spanning exon 3 and 4 junction at assay location 679 nucleotides (NM-003725.2). Human DHRS9 primers and probe (Hs00608375-m1, Applied Biosytems) result in a 66 base pair amplicon spanning exon 3 and 4 junction at assay location nucleotide 872 (NM-199204.1). PCR reactions (20 µL) contained cDNA prepared from 0.04 µg total RNA for 17β-HSD6 and RDH5 mRNA, and 0.4 µg total RNA for DHRS9 and peptidylprolyl isomerase A. cDNA was combined with 4 µL Light Cycler TaqMan Master mix (Roche) and 0.5 µL 20X TaqMan Mix (Applied Biosystems). Thermal cycler reactions were performed in triplicate and repeated twice using a Roche LightCycler at 95°C for 10 min, followed by 55 cycles at 95°C for 15 sec, 60°C for 25 sec and 72°C for 1 sec. mRNA copy number was calculated based on CT value of 21.85 for 4×10^5 copies with an amplification efficiency of 2 normalized by total RNA in the reaction.

Liquid chromatography tandem mass spectrometry

Liquid chromatography tandem mass spectrometry analysis of DHT, androstanediol and androsterone was performed as described (9). Cells were incubated for 48 h at 37°C with 100 nM androstanediol in serum-free, phenol red-free medium. Cells and media were collected together in triplicate and data pooled from two experiments. Deuterated 5α-androstan-17β-ol-3-one-16,16,17-d_3 (DHT-d_3) (CDN Isotopes, Pointe-Claire, Quebec, Canada) (12 ng) was added as internal standard and samples were extracted twice with 1.5 mL 9:1 chloroform:acetone. Organic layers were combined, evaporated under vacuum and concentrated using solid phase extraction carbon-18 columns (Varian, Palo Alto, CA). DHT, androstanediol and androsterone were measured using an Agilent 1100 capillary liquid chromatography system (Palo Alto, CA) coupled to an Applied Biosystems–MDS Sciex API-3000 triple quadrupole mass spectrometer (MDS Sciex, Concord, ON, Canada). Positive ions were formed via dopant-assisted atmospheric pressure photoionization (Applied Biosystems, Foster City, CA). A Phenomenex Luna C18 column (3 µm, 150×0.5 mm) and a gradient profile using mobile phase A (2 mM ammonium formate) and mobile phase B (2 mM ammonium formate in methanol) at 175 µL/min (65% to 80% at 2.25 min and 95% at 13 min) were used at 60°C. Androgen parent-product ion pairs monitored (mass to charge ratio, *m/z*) were 305.2 to 255.2 for DHT, 273.2 to 255.2 for androstanediol, 291.2 to 273.2 for androsterone, and 308.2 to 258.2 for the DHT-d_3 internal standard. DHT,

androstanediol and androsterone standards were from Sigma-Aldrich (St. Louis, MO). DHT-d_3 deuterated twice at carbon 16 and once at carbon 17 was used to quantitate androgen. Steroid concentrations were calculated based on pmol/g assuming 1000 g/L. The 10 pg limit of detection for DHT had signal to noise ratio >3, and the 50 pg limit of quantitation of DHT had signal to noise ratio >10.

RESULTS

Cell-specific AR transactivation in the presence of androstanediol

AR transactivation in the presence of testosterone, DHT or androstanediol was compared in benign and cancer-derived cell lines that included monkey kidney CV1 cells, human cervical carcinoma HeLa cells, benign human prostate-derived PWR-1E cells, and PC-3, LAPC-4 and CWR-R1 human prostate cancer cells (Fig. 1). A concentration-dependent increase in AR transcriptional activity was demonstrated in response to testosterone and DHT in all cell types subsequent to transfection of pCMV-AR and the PSA-Enh-Luc reporter gene. The minimal transactivation of the PSA enhancer after transfection with pCMV5 empty vector showed that androgen-dependent gene activation resulted from the expressed wild-type AR, with maximal luciferase activity between 0.1 to 10 nM testosterone or DHT. CWR-R1 and LAPC-4 cells appeared more responsive to low levels of testosterone and DHT (Fig. 1F).

In contrast to testosterone and DHT, there were major cell-type differences in AR transactivation with androstanediol. AR transactivation in the presence of 10 nM androstanediol was insignificant in CV1 cells, but evident in HeLa cells at 10 nM androstanediol (Figs. 1A and B). In PC-3, LAPC-4, CWR-R1 and PWR-1E cells, androstanediol was nearly equipotent with testosterone and DHT (Fig. 1C–F). AR binds androstanediol with low affinity (15), suggesting AR transactivation with androstanediol resulted from cell-specific conversion to DHT.

To investigate whether cell-specific AR transactivation in the presence of androstanediol resulted from oxidative conversion to DHT, different cell types were incubated with 100 nM androstanediol and androgen metabolites measured using mass spectrometry (Fig. 2A). Cell incubations were performed for 24 h to parallel the AR transactivation assays (Fig. 1) and for 48 h to assess metabolite stability. Low to undetectable androstanediol was measured in all cell types after 24 and 48 h (Fig. 2A). In contrast, DHT was highest in PWR-1E cells, at moderate levels in the LAPC-4, CWR-R1 and PC-3 cells, but nearly undetectable in HeLa and CV1 cells. Testosterone was undetectable (LAPC-4, PC-3 and HeLa cells) or 5-fold less than DHT (CWR-R1 cells) (not shown). Highest levels of androsterone were measured in HeLa and CV1 cells, with lower levels of androsterone in prostate-derived cells in an inverse relationship with DHT. For LNCaP and LNCaP-C4-2 cells, mass spectrometry indicated essentially undetectable levels of androstanediol, DHT, androsterone, testosterone and 5α-androstenedione after 24 and 48 h incubations with 100 nM androstanediol, consistent with the inability of androstanediol to activate AR in LNCaP cells (not shown), and with the high glucuronosyltransferase activity in LNCaP cells, an enzyme that irreversibly converts androstanediol to the sugar conjugate for excretion (16).

An additional indicator of androstanediol conversion to an active androgen was provided by the ability of 10 nM androstanediol or 0.1 nM DHT to increase the growth of LAPC-4 cells ($p < 0.001$) that contain a wild-type AR (Fig. 2B). Together the results indicate cell-specific AR transcriptional activity and prostate cancer cell growth in the presence of androstanediol results from the oxidative metabolism of androstanediol to DHT.

Cell-specific metabolism of androstanediol

Several enzymes are involved in the oxidative metabolism of androstanediol to DHT, and in the reductive conversion of androstanediol to androsterone (Fig. 3). Androstanediol is converted to DHT by oxidative 3α-HSD activity of 17β-HSD6 (17), RDH5 (18) and DHRS9 (19) (Table 1). Androstanediol is metabolized to androsterone by 17β-HSD6 and 11, and androsterone is glucuronidated for excretion (20–22).

Quantitative RT-PCR analysis of RNA from different cell types indicated higher levels of 17β-HSD6 mRNA in prostate-derived cells than DHRS9 or RDH5 mRNA (Fig. 4A), which correlated directly with AR transactivation and DHT levels after incubation with androstanediol (Figs. 1 and 2A). 17β-HSD6 mRNA levels were lowest in CV1 cells, where AR was transcriptionally inactive with androstanediol. HeLa cell 17β-HSD6 mRNA levels were ~7-fold greater, consistent with the increase in AR activity with 10 nM androstanediol. Highest levels of 17β-HSD6 mRNA were in PWR-1E and RWPE-2 benign prostate cells, and in LNCaP, LNCaP-C4-2, CWR-R1 and DU145 prostate cancer cells, where AR transactivation with androstanediol was similar to testosterone or DHT. In contrast, DHRS9 and RDH5 mRNA levels were lower than 17β-HSD6 mRNA (Fig. 4A) and did not correlate with DHT levels or AR transactivation with androstanediol. RDH5 mRNA levels were ~4-fold higher in CWR-R1 cells than other cell types. However, this increase was not associated with a shift in dose response of AR activity with androstanediol relative to other prostate cancer cells (Fig. 1).

Higher levels of 17β-HSD6 mRNA in prostate-derived cell lines where AR activity was greatest in response to androstanediol were also associated with higher levels of 17β-HSD6 protein (Fig. 4B). The ~30 kDa 17β-HSD6 protein was detected in all prostate-derived cell lines, but not in CV1 or HeLa cells which had correspondingly lower levels of 17β-HSD6 mRNA and AR was less active with androstanediol. AR protein levels were higher in LAPC-4, CWR-R1 and LNCaP prostate cancer cells than in PC-3, PWR-1E, HeLa or CV1 cells (Fig. 4B). Longer exposure of the transblot revealed low levels of 17β-HSD6 in HeLa cells and AR in PWR-1E cells (not shown). However, 17β-HSD6 siRNA introduced into cells did not decrease AR transactivation in response to androstanediol due to insufficient knockdown and the contributions of other enzymes that metabolize androstanediol to DHT.

The results suggest that 17β-HSD6 contributes to androstanediol conversion to DHT in benign and malignant prostate, and bioactivation of androstanediol to DHT accounts for AR transactivation in the presence of androstanediol.

Androgen metabolism during prostate cancer progression

To investigate whether enzymes involved in DHT biosynthesis in prostate cancer tissue contribute to prostate cancer progression during androgen deprivation therapy, mRNA levels for 17β-HSD6, DHRS9 and RDH5 were determined in the CWR22 xenograft at different times after castration. The CWR22 human prostate cancer xenograft undergoes remission after castration and regrowth ~120 days after castration and thus mimics the clinical response to androgen deprivation (23,24). 17β-HSD6, DHRS9 and RDH5 mRNA levels varied in the CWR22 xenograft depending upon time after castration (Fig. 5A). 17β-HSD6 mRNA levels decreased ~5-fold within 2 days after castration and remained low throughout castration-recurrent tumor growth. DHRS9 and RDH5 mRNA levels increased transiently after castration, but were unchanged in the castration-recurrent xenograft CWR22 tumor relative to the tumor prior to castration.

The decline in 17β-HSD6 mRNA after castration in the CWR22 xenograft was investigated further using androgen-stimulated benign prostate and androgen-stimulated and castration-recurrent prostate cancer tissue. Similar to results with the CWR22 prostate cancer

xenograft, 17β-HSD6 mRNA levels were highest in benign prostate, more variable in androgen-stimulated prostate cancer, and declined ~10-fold in most specimens of castration-recurrent prostate cancer (Fig. 5B).

In vivo metabolism of androstanediol to DHT

To obtain further evidence for the in vivo intratumoral metabolism of androstanediol to DHT, castrated CWR22R-bearing athymic mice were injected subcutaneously in oil at the tumor site with 1 mg androstanediol dipropionate. Intratumoral DHT measured 48 h later using tandem mass spectrometry (Table 2) was 28-fold higher (28.1 ± 6.2 nM DHT) after administering androstanediol dipropionate than control tumor-bearing mice injected with vehicle (1.0 ± 0.7 nM DHT). Androsterone levels increased 4.3-fold after injection of androstanediol dipropionate. Androstanediol was not detected in control or treated animals, consistent with its metabolism to DHT and androsterone. The results demonstrate intraprostatic tumoral metabolism of androstanediol to DHT may contribute to AR transactivation and prostate cancer progression.

DISCUSSION

Androstanediol as an active androgen precursor

The metabolic processes that contribute to castration-recurrent prostate cancer appear to be diverse, as reflected by an apparent wide variation in mechanisms and tissue androgen levels. On the other hand, AR continues to be a focus for new drug development to achieve sustained inhibition or eradication of prostate cancer growth during prolonged androgen deprivation therapy. AR activity depends on high affinity binding of testosterone or DHT, whose steady state levels are regulated by a family of reductive and oxidative enzymes (Table 1). The major circulating androgen testosterone synthesized in the testis from 4-androsten-3,17-dione (androstenedione) by reductive 17β-HSD (25) (Fig. 3,Table 1) is irreversibly converted to DHT by type 2 steroid 5α-reductase (20) that also converts androstenedione, a major adrenal androgen, to 5α-androstane-3,17-dione. Androstanedione is reversibly converted to DHT by 17β-HSD, or indirectly through androsterone and androstanediol (26). DHT is reversibly inactivated by conversion to androstanediol by reductive 3α-HSD activity (21,27) of type 3 3α-HSD aldo-keto reductase 1C2 (AKR1C2) that functions as both 3- and 17-ketosteroid reductase (19,28–30). The 17β-HSD activity of AKR1C3 converts androstanediol to androsterone, and androstenedione to testosterone (28,31). Increased levels of AKR1C ketosteroid reductases were associated with castration-recurrent prostate cancer (32). Androstanediol is metabolized by oxidative 17β-HSD activity of 17β-HSD6 and 17β-HSD11 to androsterone, which is glucuronidated and excreted (20–22).

In some prostate cancers, gain-of-function AR mutations may account for androstanediol activation of AR and increased cell growth (4,33). However, most prostate cancers retain wild-type AR that is transcriptionally inactive when bound to androstanediol (15). Alternative mechanisms for prostate cancer tissue DHT production during androgen deprivation therapy are supported by the lower levels of DHT in prostate after treatment with the type 2 5α-reductase inhibitor, finasteride (34), although some evidence suggests an increase in 5α-reductase type 1 activity (35). Treatment with the dual type 1 and type 2 5α-reductase inhibitor dutasteride decreased prostate tissue DHT from 11.5 to 0.8 nM, with a compensatory increase from 0.2 to 11.8 nM testosterone (36).

The biological significance of the back conversion of androstanediol to DHT is supported by androstanediol-induced prostate growth in beagle dogs (37), conversion of androstanediol to DHT in humans (38), and androstanediol-induced masculinization of the tammar wallaby

(39,40). Conversion of androstanediol to DHT has been attributed to several oxidative 3α-HSD enzymes. These enzymes include retinol dehydrogenase 4 (RoDH4) and RDH5 (18), 17β-HSD6 (18,19) and 10 (54) and DHRS9 (19,42) (Table 1). These hydroxysteroid dehydrogenases oxidize or reduce the 3 or 17 ketone group of androgens, with a preference for oxidization of the 3 ketone that contributes to androstanediol oxidation to androsterone. 17β-HSD6 functions primarily as a 3α-hydroxysteroid oxidoreductase that converts androstanediol to DHT, and lacks stereospecificity in the reductive direction (17). 17β-HSD6 is expressed predominantly in stromal cells at higher levels than RoDH4 or RDH5, and is considered a predominant enzyme in androstanediol conversion to DHT in human prostate (19,29). A mitochondrial 17β-HSD10 converts androstanediol to DHT in prostate tissue (Table 1) (43). Androstanediol also is acted upon by glucuronosyltransferase for rapid excretion of androstanediol glucuronide as observed in LNCaP cells (16).

Our studies have shown that benign prostate and prostate cancer cells metabolize androstanediol to DHT. Administration of androstanediol dipropionate at the CWR22R tumor site caused a 28-fold increase in DHT. Androstanediol also promoted the androgen-dependent growth of LAPC-4 cells. Since androstanediol was nearly equipotent with DHT in AR transcriptional activation in most of the prostate cell lines, the results indicate that conversion of androstanediol to DHT was sufficient to activate AR.

Conversion of androstanediol to DHT by 17β-HSD6

Higher levels of DHT and lower levels of androsterone correlated in most cell lines with greater AR transactivation in the presence of androstanediol. Quantitative mRNA measurements and enzyme protein levels suggested 17β-HSD6 is a predominant multifunctional enzyme in the oxidation and reduction of 3 and 17 keto groups, and levels correlated directly with the extent of androstanediol back-conversion to DHT and AR transactivation in the presence of androstanediol.

The ability of benign and malignant prostate cells to convert androstanediol to DHT provides a mechanism for increased AR transactivation in response to adrenal-derived androgen precursors (39). De novo synthesis of DHT from progesterone is an alternative pathway involved in environmental androgen production (44) and in castration-recurrent prostate cancer (10). During androgen deprivation therapy, androstenedione is a major circulating adrenal androgen converted to DHT through testosterone. Androstanediol is not a major adrenal androgen. However, 5α-reductase type 1 is expressed in rat adrenal and levels increased after androgen withdrawal (45). This raises the possibility that 5α-reductase type 1 can convert adrenal 17α-hydroxyprogesterone to 17α-hydroxy-dihydroprogesterone, an androstanediol precursor (46). Adrenal androstanediol also may derive from the metabolism of androstenedione to androstanedione by 5α-reductase type 1, the conversion of androstanedione to androsterone, and androsterone to androstanediol by AKR1C3 (32). Increased availability of adrenal androstanediol in patients undergoing androgen deprivation therapy could provide the substrate necessary for conversion of androstanediol to DHT by 17β-HSD6.

Enzyme activity depends ultimately on mRNA and protein levels. Measurements of 17β-HSD6 mRNA and protein levels in prostate cancer cell lines correlated well with AR transactivation in response to androstanediol, and with the conversion of androstanediol to DHT based on mass spectrometry measurements. However, hydroxysteroid dehydrogenase activities also depend on the levels of oxidized and reduced NAD/H and NADP/H (43).

Our studies suggest that 17β-HSD6 is one of several enzymes involved in the peripheral conversion of androstanediol to DHT in prostate. 17β-HSD6 mRNA levels declined 5 to 10-fold in the castration-recurrent CWR22 and clinical specimens compared to androgen-

stimulated prostate cancer, and did not rebound with castration-recurrent tumor growth. The decline in 17β-HSD6 mRNA in prostate cancer tissue after castration is consistent with the ~ 90% decline in DHT to levels that remain sufficient to activate AR (8,9). DHT levels may also decrease because of less 5α-reduction (35). In contrast, DHRS9 and RDH5 mRNA levels increased transiently after castration in the CWR22 tumor, but were similar in the androgen-stimulated and castration-recurrent CWR22 xenografts. The results contrast with a recent report that suggested a slight increase in RDH5 mRNA levels in the LNCaP xenograft upon progression to castration-recurrent growth (10).

Unlike DHT, testosterone persists in the normal range in castration-recurrent prostate cancer tissue (8,9) from local tissue production and from adrenal androgen conversion such as from dehydroepiandrosterone in stromal cells (47). Testosterone may serve a greater role in AR transactivation in castration-recurrent prostate cancer growth through mechanisms that include increased levels of AR coactivators (6,7) and, in uncommon cases, AR somatic mutants such as AR-H874Y that increase testosterone-dependent AR transcriptional activity to levels similar to DHT (1,48). However, our studies suggest that testosterone was not a major metabolite of androstanediol metabolism to DHT.

Clinical relevance and conclusions

The importance of local active androgen production in prostate cancer growth during androgen deprivation therapy has gained renewed attention. Prostate tissue DHT persists after castration at levels approximately 10% of normal, with higher levels of testosterone (8–10,49–51). Steroid 5α-reductase levels increase in androgen-stimulated benign prostate and prostate cancer (52), and a shift from steroid 5α-reductase type 2 toward type 1 contributes to the conversion of testosterone to DHT in prostate cancer (35). The prevalence of prostate cancer progression during androgen deprivation therapy by medical or surgical castration suggests mechanisms independent of AR may contribute to prostate cancer growth. However, inhibition of prostate cancer growth by reducing AR levels indicates that AR is a critical mediator of castration-recurrent growth (2). In agreement with these findings, a phase I clinical trial using abiraterone acetate, a selective steroid 17α-hydroxylase (CPY17) inhibitor, reduced PSA levels (53), which suggests that ligand-activated AR contributes to castration-recurrent prostate cancer growth. We have shown that prostate-derived cells and tissues express steroid metabolic enzymes important in DHT synthesis that maintain AR-dependent gene transcription to a greater extent than in cells from other organs. AR may be transcriptionally active in castration-recurrent prostate cancer through local bioactivation of androstanediol to DHT by 17β-HSD6. The acquired capacity of prostate cancer cells to produce testosterone and DHT from androgen precursors and catabolites establishes an environment for AR stimulation of recurrent growth during androgen deprivation therapy.

Acknowledgments

Supported by National Cancer Institute Center Grant P01-CA77739 (JLM and EMW) and Cancer Center Support Grant to Roswell Park Cancer Institute CA16156 (JLM), University of North Carolina at Chapel Hill Lineberger Cancer Center CA34026 (JLM), and US Public Health Service Grants HD16910 from the National Institute of Child Health and Human Development (EMW) and by the Intramural Program of the NIH, National Institute of Environmental Health Sciences (Z01 ES5050167) (KBT).

REFERENCES

1. Askew EB, Gampe RT, Stanley TB, Faggart JL, Wilson EM. Modulation of androgen receptor activation function 2 by testosterone and dihydrotestosterone. J Biol Chem. 2007; 282:25801–25816. [PubMed: 17591767]

2. Zegarra-Moro OL, Schmidt LJ, Huang H, Tindall DJ. Disruption of androgen receptor function inhibits proliferation of androgen-refractory prostate cancer cells. Cancer Res. 2002; 62:1008–1013. [PubMed: 11861374]
3. Linja MJ, Savinainen KJ, Saramäki OR, Tammela TL, Vessella RL, Visakorpi T. Amplification and overexpression of androgen receptor gene in hormone-refractory prostate cancer. Cancer Res. 2001; 61:3550–3555. [PubMed: 11325816]
4. Steketee K, Timmerman L, Ziel-van der Made AC, Doesburg P, Brinkmann AO, Trapman J. Broadened ligand responsiveness of androgen receptor mutants obtained by random amino acid substitution of H874 and mutation hot spot T877 in prostate cancer. Int J Cancer. 2002; 100:309–317. [PubMed: 12115546]
5. Tan J, Sharief Y, Hamil KG, et al. Dehydroepiandrosterone activates mutant androgen receptors expressed in the androgen-dependent human prostate cancer xenograft CWR22 and LNCaP cells. Mol Endocrinol. 1997; 11:450–459. [PubMed: 9092797]
6. Gregory CW, He B, Johnson RT, et al. A mechanism for androgen receptor-mediated prostate cancer recurrence after androgen deprivation therapy. Cancer Res. 2001; 61:4315–4319. [PubMed: 11389051]
7. Karpf AR, Bai S, James SR, Mohler JL, Wilson EM. Increased expression of androgen receptor coregulator MAGE-11 in prostate cancer by DNA hypomethylation and cyclic AMP. Mol Cancer Res. 2009; 7:523–535. [PubMed: 19372581]
8. Mohler JL, Gregory CW, Ford OH 3rd, Kim D, Weaver CM, Petrusz P, Wilson EM, French FS. The androgen axis in recurrent prostate cancer. Clin Can Res. 2004; 10:440–448.
9. Lih FB, Titus MA, Mohler JL, Tomer KB. Atmospheric pressure photoionization tandem mass spectrometry of androgens in prostate cancer. Anal Chem. 2010; 82:6000–6007. [PubMed: 20560527]
10. Locke JA, Guns ES, Lubik AA, et al. Androgen levels increase by intratumoral de novo steroidogenesis during progression of castration-resistant prostate cancer. Cancer Res. 2008; 68:6407–6415. [PubMed: 18676866]
11. Wang G, Sadar MD. Amino-terminus domain of the androgen receptor as a molecular target to prevent the hormonal progression of prostate cancer. J Cell Biochem. 2006; 98:36–53. [PubMed: 16440300]
12. Harper ME, Pike A, Peeling WB, Griffiths K. Steroids of adrenal origin metabolized by human prostatic tissue both in vivo and in vitro. J Endocrinol. 1974; 60:117–125. [PubMed: 4130214]
13. Gregory CW, Johnson RT, Mohler JL, French FS, Wilson EM. Androgen receptor stabilization in recurrent prostate cancer is associated with hypersensitivity to low androgen. Cancer Res. 2001; 61:2892–2898. [PubMed: 11306464]
14. Bai S, Grossman G, Yuan L, et al. Hormone control and expression of androgen receptor coregulator MAGE-11 in human endometrium during the window of receptivity to embryo implantation. Mol Hum Reprod. 2008; 14:107–116. [PubMed: 18048459]
15. Penning TM. Molecular endocrinology of hydroxysteroid dehydrogenases. Endocr Rev. 1997; 18:281–305. [PubMed: 9183566]
16. Guillemette C, Hum DW, Bélanger A. Specificity of glucuronosyltransferase activity in the human cancer cell line LNCaP, evidence for the presence of at least two glucuronosyltransferase enzymes. J Steroid Biochem Mol Biol. 1995; 55:355–362. [PubMed: 8541232]
17. Chetyrkin SV, Hu J, Gough WH, Dumaual N, Kedishvili NY. Further characterization of human microsomal 3alpha-hydroxysteroid dehydrogenase. Arch Biochem Biophys. 2001; 386:1–10. [PubMed: 11360992]
18. Biswas MG, Russell DW. Expression cloning and characterization of oxidative 17beta- and 3alpha-hydroxysteroid dehydrogenases from rat and human prostate. J Biol Chem. 1997; 272:15959–15966. [PubMed: 9188497]
19. Bauman DR, Steckelbroeck S, Williams MV, Peehl DM, Penning TM. Identification of the major oxidative 3alpha-hydroxysteroid dehydrogenase in human prostate that converts 5α-androstane-3α, 17β-diol to 5α-dihydrotestosterone: a potential therapeutic target for androgen-dependent disease. Mol Endocrinol. 2006; 20:444–458. [PubMed: 16179381]

20. Russell DW, Wilson JD. Steroid 5 alpha-reductase: two genes/two enzymes. Annu Rev Biochem. 1994; 63:25–61. [PubMed: 7979239]
21. Bartsch W, Klein H, Schiemann U, Bauer HW, Voigt KD. Enzymes of androgen formation and degradation in the human prostate. Ann NY Acad Sci. 1990; 595:53–66. [PubMed: 1695829]
22. Beaulieu M, Lévesque E, Hum DW, Bélanger A. Isolation and characterization of a novel cDNA encoding a human UDP-glucuronosyltransferase active on C19 steroids. J Biol Chem. 1996; 271:22855–22862. [PubMed: 8798464]
23. Nagabhushan M, Miller CM, Pretlow TP, et al. CWR22: the first human prostate cancer xenograft with strongly androgen-dependent and relapsed strains both in vivo and in soft agar. Cancer Res. 1996; 56:3042–3046. [PubMed: 8674060]
24. Kim D, Gregory CW, French FS, Smith GJ, Mohler JL. Androgen receptor expression and cellular proliferation during transition from androgen-dependent to recurrent growth after castration in the CWR22 prostate cancer xenograft. Am J Pathol. 2002; 160:219–226. [PubMed: 11786415]
25. Geissler WM, Davis DL, Wu L, et al. Male pseudohermaphroditism caused by mutations of testicular 17 beta-hydroxysteroid dehydrogenase 3. Nat Genet. 1994; 7:34–39. [PubMed: 8075637]
26. Weisser H, Krieg M. Kinetic analysis of androstenedione 5 alpha-reductase in epithelium and stroma of human prostate. Steroids. 1997; 62:589–594. [PubMed: 9432753]
27. Span PN, Sweep CG, Benraad TJ, Smals AG. 3 Alpha-hydroxysteroid oxidoreductase activities in dihydrotestosterone degradation and back-formation in rat prostate and epididymis. J Steroid Biochem Mol Biol. 1996; 58:319–324. [PubMed: 8836171]
28. Penning TM, Steckelbroeck S, Bauman DR, et al. Aldo-keto reductase (AKR) 1C3: role in prostate disease and the development of specific inhibitors. Mol Cell Endocrinol. 2006; 248:182–191. [PubMed: 16417966]
29. Penning TM, Bauman DR, Jin Y, Rizner TL. Identification of the molecular switch that regulates access of 5alpha-DHT to the androgen receptor. Mol Cell Endocrinol. 2007; 265–266:77–82.
30. Cooper WC, Jin Y, Penning TM. Elucidation of a complete kinetic mechanism for a mammalian hydroxysteroid dehydrogenase (HSD) and identification of all enzyme forms on the reaction coordinate: the example of rat liver 3alpha-HSD (AKR1C9). J Biol Chem. 2007; 282:33484–33493. [PubMed: 17848571]
31. Lin HK, Jez JM, Schlegel BP, Peehl DM, Pachter JA, Penning TM. Expression and characterization of recombinant type 2 3 alpha-hydroxysteroid dehydrogenase (HSD) from human prostate: demonstration of bifunctional 3 alpha/17 beta-HSD activity and cellular distribution. Mol Endocrinol. 1997; 11:1971–1984. [PubMed: 9415401]
32. Stanbrough M, Bubley GJ, Ross K, et al. Increased expression of genes converting adrenal androgens to testosterone in androgen-independent prostate cancer. Cancer Res. 2006; 66:2815–2825. [PubMed: 16510604]
33. Mizokami A, Koh E, Fujita H, et al. The adrenal androgen androstenediol is present in prostate cancer tissue after androgen deprivation therapy and activates mutated androgen receptor. Cancer Res. 2004; 64:765–771. [PubMed: 14744796]
34. Stoner E. The clinical development of a 5 alpha-reductase inhibitor, finasteride. J Steroid Biochem Mol Biol. 1990; 37:375–378. [PubMed: 1701660]
35. Titus MA, Gregory CW, Ford OH, Schell MJ, Maygarden SJ, Mohler JL. Steroid 5alpha-reductase isozymes I and II in recurrent prostate cancer. Clin Cancer Res. 2005; 11:4365–4371. [PubMed: 15958619]
36. Mostaghel EA, Geng L, Holcomb I, Coleman IM, Lucas J, True LD, Nelson PS. Variability in the androgen response of prostate epithelium to 5alpha-reductase inhibition: implications for prostate cancer chemoprevention. Cancer Res. 2010; 70:1286–1295. [PubMed: 20124490]
37. Walsh PC, Wilson JD. The induction of prostatic hypertrophy in the dog with androstanediol. J Clin Invest. 1976; 57:1093–1097. [PubMed: 59740]
38. Kinouchi T, Horton R. 3Alpha-androstanediol kinetics in man. J Clin Invest. 1974; 54:646–653. [PubMed: 4855449]

39. Shaw G, Fenelon J, Sichlau M, Auchus RJ, Wilson JD, Renfree MB. Role of the alternate pathway of dihydrotestosterone formation in virilization of the Wolffian ducts of the tammar wallaby, Macropus eugenii. Endocrinology. 2006; 147:2368–2373. [PubMed: 16469812]
40. Shaw G, Renfree MB, Leihy MW, Shackleton CH, Roitman E, Wilson JD. Prostate formation in a marsupial is mediated by the testicular androgen 5 alpha-androstane-3 alpha,17 beta-diol. Proc Natl Acad Sci USA. 2000; 97:12256–12259. [PubMed: 11035809]
41. Bauman DR, Steckelbroeck S, Peehl DM, Penning TM. Transcript profiling of the androgen signal in normal prostate, benign prostatic hyperplasia, and prostate cancer. Endocrinology. 2006; 147:5806–5816. [PubMed: 16959841]
42. Balk, SP. Increased expression of genes converting adrenal androgens to testosterone in castration-recurrent prostate cancer. In: Tindall, D.; Mohler, JL., editors. Androgen action in prostate cancer. New York: Springer; 2009. p. 123-139.
43. Yang H, Yang T, Baur JA, et al. Nutrient-sensitive mitochondrial NAD+ levels dictate cell survival. Cell. 2007; 130:1095–1107. [PubMed: 17889652]
44. Carson JD, Jenkins RL, Wilson EM, Howell WM, Moore R. Naturally occurring progesterone in Loblolly pine (*Pinus Taeda L.*): a major steroid precursor of environmental androgens. Environ Toxicol Chem. 2008; 27:1273–1278. [PubMed: 18229975]
45. Yokoi H, Tsuruo Y, Miyamoto T, Ishimura K. Steroid 5 alpha-reductase type 1 immunolocalized in the adrenal gland of normal, gonadectomized, and sex hormone-supplemented rats. Histochem Cell Biol. 1998; 109:127–134. [PubMed: 9504773]
46. Auchus RJ. Non-traditional metabolic pathways of adrenal steroids. Rev Endocr Metab Disord. 2009; 10:27–32. [PubMed: 18720009]
47. Mizokami A, Koh E, Izumi K, et al. Prostate cancer stromal cells and LNCaP cells coordinately activate the androgen receptor through synthesis of testosterone and dihydrotestosterone from dehydroepiandrosterone. Endocr Relat Cancer. 2009; 16:1139–1155. [PubMed: 19608712]
48. Taplin ME, Bubley GJ, Shuster TD, et al. Mutation of the androgen-receptor gene in metastatic androgen-independent prostate cancer. N Engl J Med. 1995; 332:1393–1398. [PubMed: 7723794]
49. Salerno R, Moneti G, Forti G, et al. Simultaneous determination of testosterone, dihydrotestosterone and 5 alpha-androstan-3 alpha,-17 beta-diol by isotopic dilution mass spectrometry in plasma and prostatic tissue of patients affected by benign prostatic hyperplasia. Effects of 3-month treatment with a GnRH analog. J Androl. 1988; 9:234–240. [PubMed: 2460425]
50. Geller J, Albert JD, Nachtsheim DA, Loza D. Comparison of prostatic cancer tissue dihydrotestosterone levels at the time of relapse following orchiectomy or estrogen therapy. J Urol. 1984; 132:693–696. [PubMed: 6471215]
51. Mostaghel EA, Page ST, Lin DW, et al. Intraprostatic androgens and androgen-regulated gene expression persist after testosterone suppression: therapeutic implications for castration-resistant prostate cancer. Cancer Res. 2007; 67:5033–5041. [PubMed: 17510436]
52. Silver RI, Wiley EL, Davis DL, Thigpen AE, Russell DW, McConnell JD. Expression and regulation of steroid 5 alpha-reductase 2 in prostate disease. J Urol. 1994; 152:433–437. [PubMed: 7516976]
53. Attard G, Reid AH, Yap TA, et al. Phase I clinical trial of a selective inhibitor of CYP17, abiraterone acetate, confirms that castration-resistant prostate cancer commonly remains hormone driven. J Clin Oncol. 2008; 26:4563–4571. [PubMed: 18645193]
54. He XY, Yang YZ, Peehl DM, Lauderdale A, Schulz H, Yang SY. Oxidative 3alpha-hydroxysteroid dehydrogenase activity of human type 10 17beta-hydroxysteroid dehydrogenase. J Steroid Biochem Mol Biol. 2003; 87:191–198. [PubMed: 14672739]
55. Brereton P, Suzuki T, Sasano H, et al. Pan1b (17betaHSD11)-enzymatic activity and distribution in the lung. Mol Cell Endocrinol. 2001; 171:111–117. [PubMed: 11165019]

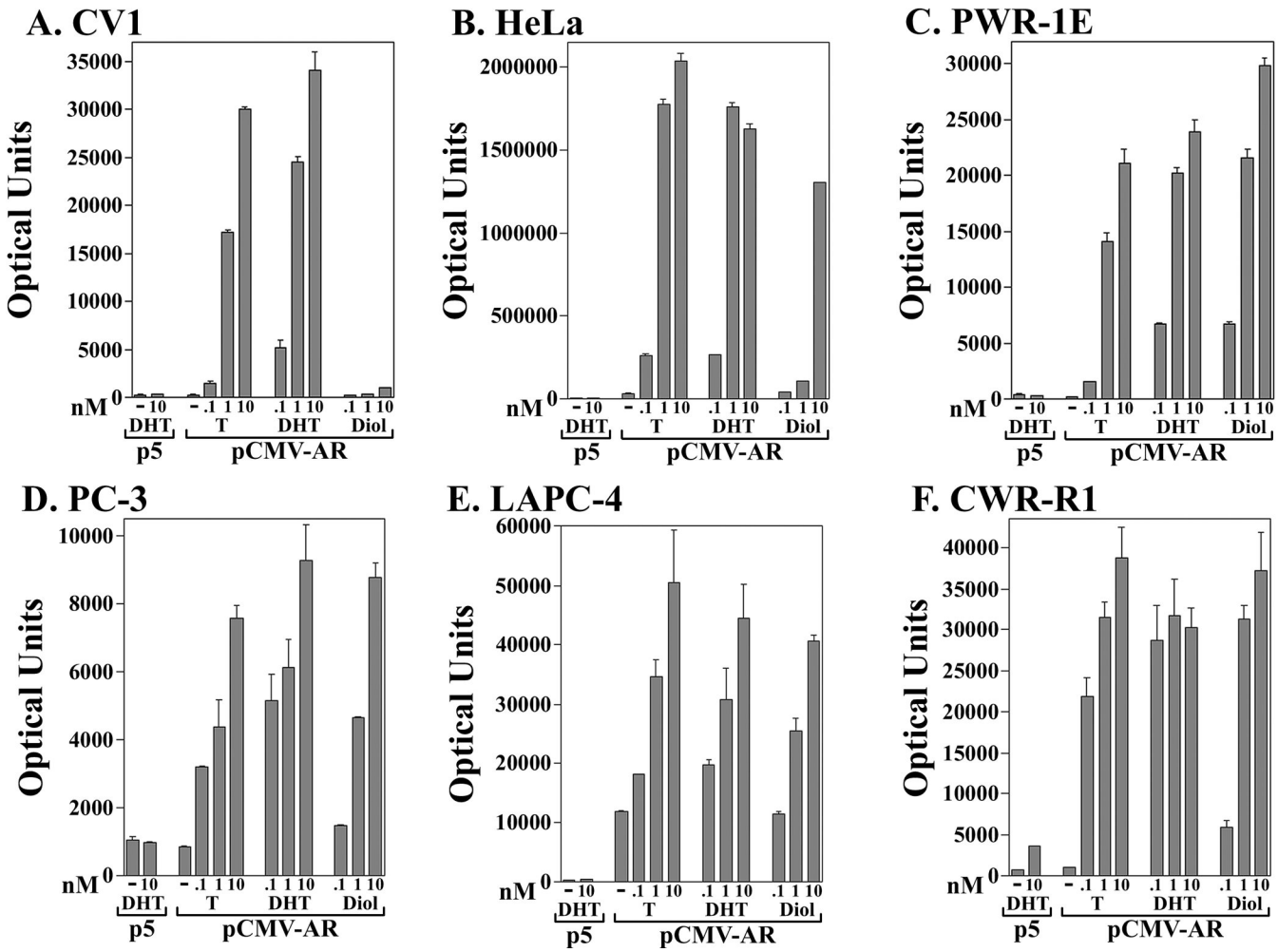

Figure 1. Cell-specific wild-type AR transactivation in the presence of androstanediol

(**A**) CV1, (**B**) HeLa, (**C**) PWR-1E, (**D**) PC-3, (**E**) LAPC-4 and (**F**) CWR-R1 cells were transfected as described in Methods with pCMV5 empty vector (p5) or pCMV-AR and PSA-Enh-Luc and incubated for 24 h in serum-free, phenol red-free medium in the absence and presence of increasing concentrations of testosterone (T), DHT and androstanediol (Diol). Luciferase activity measurements indicating the mean ± S.E. are representative of at least three independent experiments.

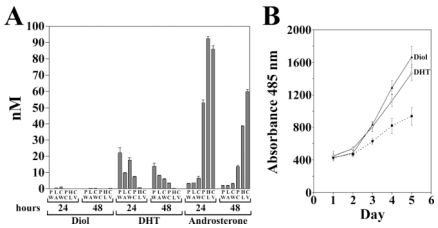

Figure 2. Androstanediol metabolism to DHT increases LAPC-4 cell growth

(**A**) PWR-1E (PW), LAPC-4 (LA), CWR-R1 (CW), PC-3 (PC), HeLa (HL), and CV1 (CV) cells were incubated in serum-free, phenol red-free medium containing 100 nM androstanediol for 24 and 48 h at 37°C. Steroids were extracted from cells and medium and quantitated using mass spectrometry. Shown are the nM concentrations of androstanediol (Diol), DHT and androsterone. (**B**) LAPC-4 cell growth assays were performed as described in Methods. Cells were incubated without hormone (- -) or with 0.1 nM DHT (O) or 10 nM androstanediol (▲). Assays performed in triplicate are the mean ± SE of duplicate experiments.

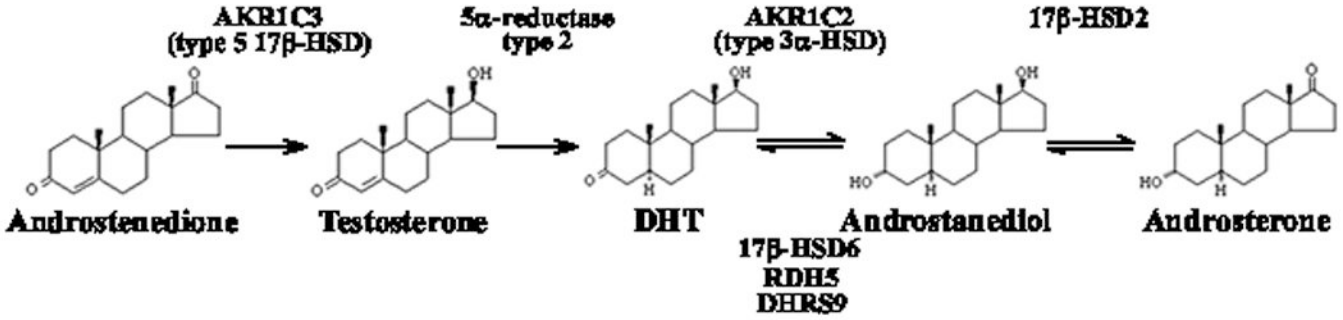

Figure 3. Schematic diagram of DHT metabolism

Androstenedione is metabolized to testosterone in peripheral tissues by aldo-keto reductase 1C3 (AKR1C3). 5α-reductase type 2 irreversibly converts testosterone to DHT which is 3-keto reduced reversibly to the inactive metabolite androstanediol by the aldo-keto reductase 1C2 (AKR1C2). Androstanediol is oxidized to DHT by 17β-hydroxysteroid dehydrogenase 6 (17β-HSD6), retinol dehydrogenase 5 (RDH5) and dehydrogenase/reductase short-chain dehydrogenase/reductase family member 9 (DHRS9). Androstanediol is oxidized reversibly to androsterone by 17β-HSD6 and 11.

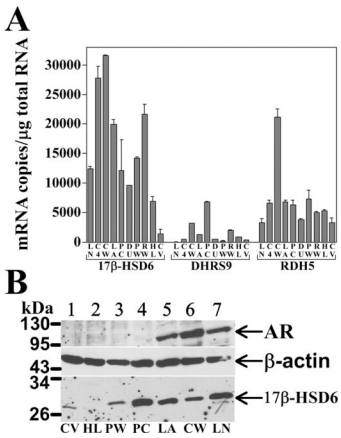

Figure 4. Cell-specific expression of 17β-HSD6, DHRS9 and RDH5 mRNA and 17β-HSD6 protein expression in different cell lines

(**A**) RNA was analyzed by quantitative RT-PCR from LNCaP (LN), LNCaP-C4-2 (C4), CWR-R1 (CW), LAPC-4 (LA), PC-3 (PC), DU145 (DU), PWR-1E (PW), RWPE-2 (RW), HeLa (HL) and CV1 cells (CV) for 17β-HSD6, DHRS9 and RDH5. (**B**) Cell extracts (150 µg protein/lane) were analyzed on immunoblots for CV1 (CV), HeLa (HL), PWR-1E (PW), PC-3 (PC), LAPC-4 (LA), CWR-R1 (CW) and LNCaP (LN) cells. The upper panel was probed with AR32 and AR52 antibodies, and the lower portion with 17β-HSD6 rabbit polyclonal antibody, and stripped and reprobed with mouse β-actin antibody.

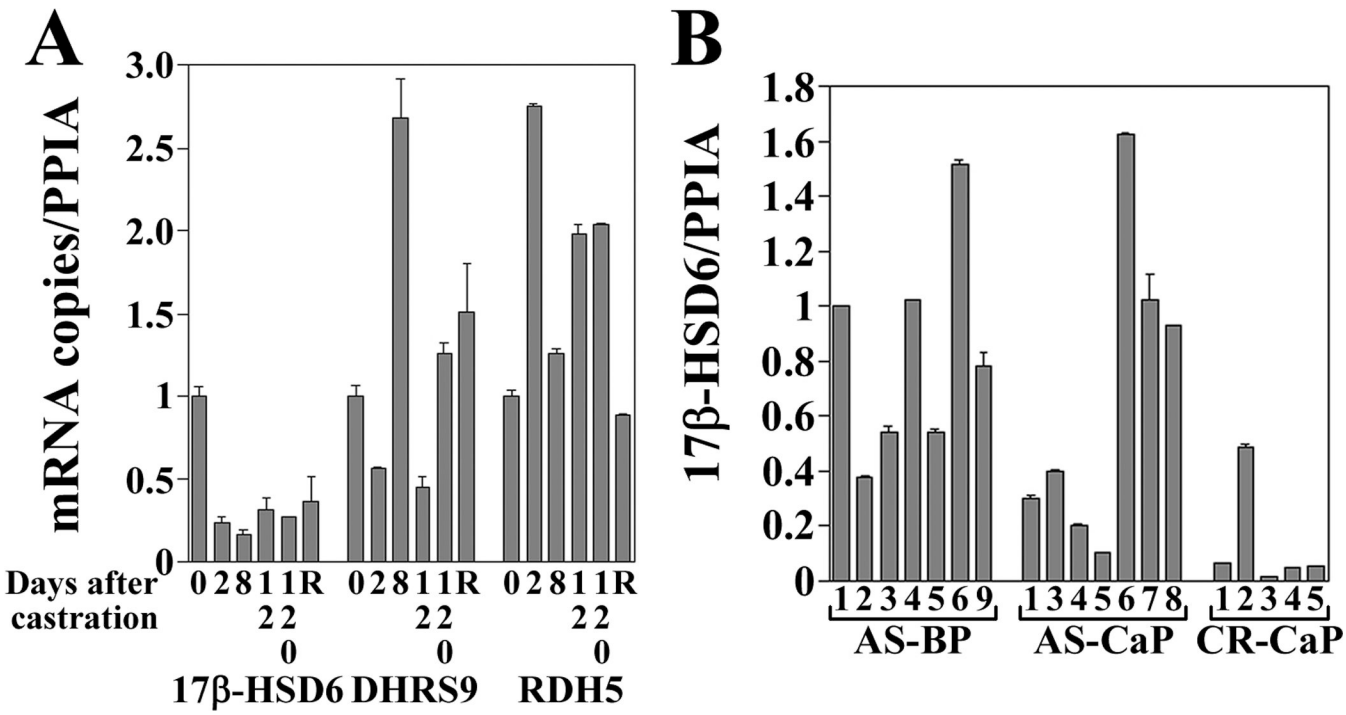

Figure 5. 17β-HSD6, DHRS9 and RDH5 mRNA levels in the CWR22 xenograft before and after castration and 17β-HSD6 mRNA levels in benign and malignant prostate

(**A**) RNA was extracted from CWR22 tumors before castration (0) and 2, 8, 12 and 120 days after castration, and from the castration-recurrent tumor > 120 days after castration (R). mRNA was measured using quantitative PCR for 17β-HSD6, DHRS9 and RDH5 and expressed as mRNA copies relative to peptidylprolyl isomerase A (PPIA) ± S.E. (**B**) 17β-HSD mRNA levels were determined relative to PPIA for individual patient samples using quantitative PCR for androgen-stimulated benign prostate (AS-BP) (1–6 and 9), androgen-stimulated prostate cancer (AS-CaP) (1 and 3–8), and castration-recurrent prostate cancer (CR-CaP) (1–5).

Table 1
Major enzymes of testosterone (T) and dihydrotestosterone (DHT) metabolism

Steroid conversion	Enzyme activity	Enzyme Acronym	Reference
	Reductive 17β-HSD activity		
Androstenedione → T	17β-hydroxysteroid dehydrogenase (RED)	17β-HSD3, 17β-HSD5	25,28
	3α-HSD aldo-keto reductase 1C3	AKR1C3	28,31
	5α-reductase activity		
T → DHT **Androstenedione → Androstanedione**	steroid 5α-reductase type 1, 2	SRD5A1, SRD5A2	20
	steroid 5α-reductase type 1, 2	SRD5A1, SRD5A2	26
	Reductive 3α-HSD activity		
DHT → Androstanediol	3α-hydroxysteroid dehydrogenase (RED)	3α-HSD	27
	type 3 3α-HSD aldo-keto reductase 1C2	AKR1C2	19,30
Androstanediol → DHT	**Oxidative 3α-HSD activity**		
	17β-hydroxysteroid dehydrogenase 6	17β-HSD6, RoDH-like 3α-HSD, RL-HSD	18,19
	17β-hydroxysteroid dehydrogenase 10	17β-HSD10	54
	retinol dehydrogenase 4	RoDH4	18
	retinol dehydrogenase 5	RDH5, 11-cis-retinol dehydrogenase, RoDH5	18
	dehydrogenase short-chain reductase family member 9	DHRS9, 3α-HSD	19,42
Androstanediol → Androsterone	**Oxidative 17β-HSD activity**		
	17β-hydroxysteroid dehydrogenase 6	17β-HSD6	18,19
	17β-hydroxysteroid dehydrogenase 11	17β-HSD11	55

Table 2

DHT, androsterone and androstanediol in CWR22R xenografts of animals treated with or without androstanediol dipropionate

Athymic nude mice bearing the CWR22R human prostate xenograft were injected subcutaneously at the tumor site with vehicle (control, left panel) or 1 mg androstanediol dipropionate (Diol-dipro, right panel). Tumors were harvested 48 h later and androgen levels (nM ± standard error of mean, SEM) determined using mass spectrometry. Androstanediol (Diol) was below the limit of detection (LOD) in tumors from control and treated mice, and DHT and androsterone (AND) was below the limit of quantitation (LOQ) in some tumors from control animals. DHT ($p = 0.003$) and AND ($p = 0.0033$) mean levels were different in control and treated groups using the nonparametric Mann-Whitney test.

Control	DHT (nM)	AND (nM)	Diol (nM)		Diol-dipro	DHT (nM)	AND (nM)	Diol (nM)
1	1.6	3.0	<LOD		1	22.7	6.7	<LOD
2	3.6	2.9	<LOD		2	30.4	7.4	<LOD
3	<LOQ	<LOQ	<LOD		3	16.9	3.6	<LOD
4	<LOQ	2.4	<LOD		4	32.7	6.7	<LOD
5	<LOQ	1.6	<LOD		5	54.5	30.4	<LOD
Mean	1.0	2.0	N/A		6	27.6	13.0	<LOD
SEM	0.7	0.6	N/A		7	11.9	5.3	<LOD
					Mean	28.1	10.4	N/A
					SEM	6.2	4.1	N/A